J. F. Flavenot and N. Skalli**

A Critical Depth Criterion for the Evaluation of Long-Life Fatigue Strength under Multiaxial Loading and a Stress Gradient

REFERENCE Flavenot, J. F. and Skalli, N., **A critical depth criterion for the evaluation of long-life fatigue strength under multiaxial loading and a stress gradient,** *Biaxial and Multiaxial Fatigue*, EGF 3 (Edited by M. W. Brown and K. J. Miller), 1989, Mechanical Engineering Publications, London, pp. 355–365.

ABSTRACT An analysis of fatigue test data taken from the literature has shown the importance of a critical layer that characterizes the microstructural state of the material, and which represents the elementary volume acting during the fatigue damage process. This parameter is combined with a multiaxial fatigue criterion, so that a new intrinsic fatigue criterion is obtained for the material, allowing the computation of fatigue life of notched parts under multiaxial stresses. Further experimental work is needed to fully validate this model.

Introduction

Most fatigue cracks of mechanical parts initiate in stress concentration zones where the material is simultaneously submitted to a complex state of stress and a stress gradient.

When assessing the behaviour of notched parts, for example, those submitted to multiaxial stresses, the mechanical engineer is faced with two problems. Firstly he must have a long-life fatigue criterion for the material submitted to the complex stress state, which can be determined from knowledge of mono-mode loading fatigue tests (e.g., uniaxial tension, rotating bending, etc.). Secondly he must be able to introduce into this criterion the concept of stress gradient which considerably influences fatigue behaviour. A great deal of research has been done on both aspects of this problem, but until now no general criterion can take into account both the stress gradient and the multiaxial stress state (1).

Accordingly, we present research work aimed at establishing the fundamentals of a general criterion. By analysing results of fatigue tests on notched specimens, we have been able to illustrate the importance of a critical depth to characterize the microstructural state of a material. This new parameter should be representative of the elementary volume acting during the fatigue damage process at crack initiation. Integrating this concept into a multiaxial fatigue criterion gives a general criterion which agrees well with experimental data.

* CETIM, 52 Avenue Félix Louat, 60304 – Senlis, France.

Notation

$\Delta\tau$	Shear stress range in the most unfavourably-oriented plane
$\Delta\tau_{oct}$	Octahedral shear stress range
τ_a	Shear stress amplitude calculated at the surface of the specimen
p_{max}	Maximum hydrostatic stress during the fatigue loading calculated at the surface of the specimen
$\sigma_1, \sigma_2, \sigma_3$	Principal stresses due to fatigue loading
$\sigma_{1,a}, \sigma_{2,a}, \sigma_{3,a}$	Principal stress amplitude for in-phase multiaxial loading
τ_a^*, p_{max}^*	Values of τ_a and p_{max}, respectively, calculated at the critical depth
$\overline{\tau_a}, \overline{p_{max}}$	Mean values of τ_a and p_{max}, respectively, averaged over the volume element from the surface to twice the critical depth
$\sigma_{y,c}$	Cyclic yield stress (measured on the cyclic stress-strain hardening curve)
$\alpha, \alpha', \beta, \beta'$	Material constants

Development of a fatigue criterion for multiaxial stresses and a stress gradient

The development of a long-life fatigue criterion of general validity requires taking into account several experimental considerations.

(1) The mechanism corresponding to the initiation of fatigue cracks is most often the shearing of crystallographic planes. It appears logical then to have a criterion relating the complex stress state to an alternating shear plane (Tresca criterion), or the local octahedral shear stress on a (111) plane with respect to the three main directions (von Mises criterion). Dang Van has shown that, in the case of proportional loading, this local shear has the value of the macroscopic alternating shear (**2**).

(2) The hydrostatic stress (or octahedral normal stress) strongly affects the fatigue strength. One may explain numerous test results by taking this into account (**2**).

(3) The criterion in question shall be valid in the case of proportional multiaxial loading, that is, for in-phase varying stresses, and also in the more general case of non-proportional or out-of-phase loading. For these reasons, we have selected Dang Van's (**2**) and Crossland's (**3**) criteria for the treatment of the experimental data. They are expressed by equations (1) and (2), respectively.

$$\Delta\tau + \alpha p_{max} < \beta \tag{1}$$

$$\Delta\tau_{oct} + \alpha' p_{max} < \beta' \tag{2}$$

Where τ_a is the local shear stress range in the most unfavourably-oriented plane, τ_{oct} the local octahedral shear stress range, and p_{max} the maximum hydrostatic stress of the fatigue cycle.

Both criteria are similar, and they may be used, with some modifications, in the case of general loading including non-proportional loading.

The relationship suggested by Fuchs for the von Mises criterion (4) may be used for the Crossland criterion. A more useful formulation of these criteria (Dang Van or Crossland) has recently been proposed for non-proportional loading (5).

When introducing the concept of stress gradient into a multiaxial-stress fatigue criterion, the following consideration should be taken into account: (i) the fatigue behaviour of a material does not depend only on the stress state at some particular position, and (ii) the heterogeneity of metals and the stress distribution underneath the surface on which the fatigue cracks initiate are active in any fatigue damage process. In consequence it is necessary to perform any analysis on a volume large enough to represent the true behaviour of the material. This brought about the idea of a volume or a distance which would characterize the material. About thirty years ago, Neuber (6) and Heywood (7) used a characteristic length in the definition of the fatigue notch factor K_f.

Stieler (8) suggested in 1954 the concept of a 'critical layer' in order to take into account the phenomenon of elastic shakedown at the notch tip. More recently, Devaux (9) using linear elastic fracture mechanics has shown that crack initiation is predicted with a criterion based upon a distance, d, characterizing the material. Matake and Imai (10) in order to plot torsion and bending test results calculated the mean value of stresses for half the thickness of a grain.

Moreover, the analysis of the initiation and crack growth threshold of short fatigue cracks (11)(12) has shown the important effect of grain size, and emphasized the need to take into consideration the stress state within a sufficiently large volume, or at some defined distance from the surface. These various studies show that it should be possible to determine a critical depth (layer thickness) characterizing each material, which could be used as basic information for an analysis.

The critical layer

The fatigue limits obtained during tests under tension–compression on cylindrically notched specimens (diameter 7.98 mm) have been analysed (13), using data obtained from references (14)–(17) and applying both the Dang Van and the Crossland criteria. Each geometry has been analysed by the finite element method, and the variation of the principal stresses σ_1, σ_2, and σ_3, in relation to depth has been determined (Fig. 1). Moreover, the distribution of the amplitudes of the shear stress τ_a and the maximum hydrostatic stress p_{max} have been calculated for the fatigue limit, i.e.

$$\tau_a = \frac{\sigma_{1,a} - \sigma_{3,a}}{2} \tag{3}$$

Where $\sigma_{1,a}$ and $\sigma_{2,a}$ are the amplitudes of the two extreme principal stresses, and

$$p_{max} = \frac{(\sigma_1 + \sigma_2 + \sigma_3)_{max}}{3} = \frac{\sigma_{1max} + \sigma_{2max} + \sigma_{3max}}{3} \tag{4}$$

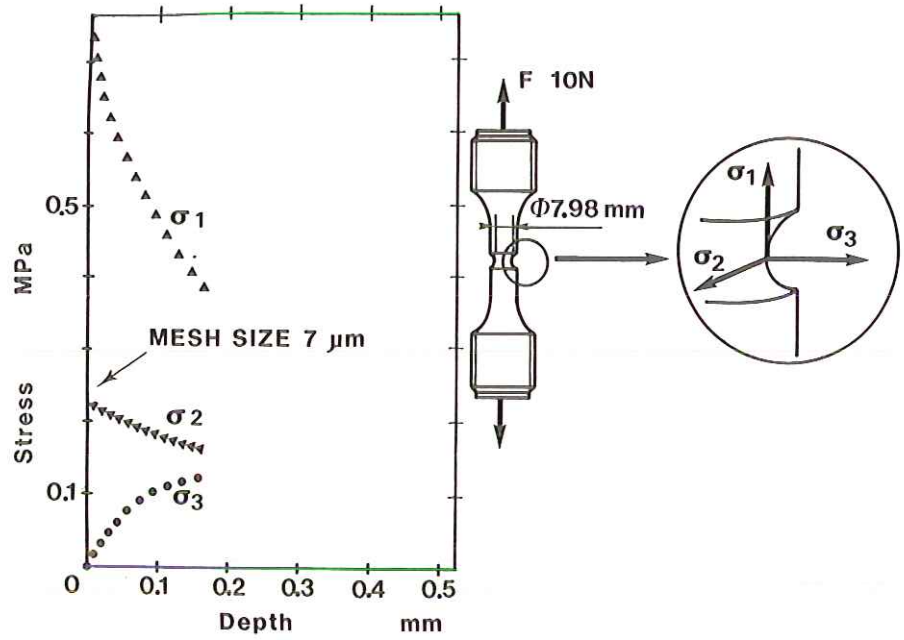

Fig 1 Distribution of principal stresses in relation to distance from the surface of a notched specimen of $K_t = 3.3$

For the tension–compression test data used here σ_{1max}, σ_{2max}, σ_{3max} are the values obtained for σ_1, σ_2, σ_3 at the maximum fatigue cycle load applied to the tensile specimen.

In order to get a very accurate distribution of stress in the neighbourhood of the notch, the finite element mesh was refined in the layer near the surface, the size of the elements being in the range 7–15 μm (6-node isoparametric triangular elements). The stress is linearly extrapolated from gauss points to nodes, and then averaged. Convergence tests have been made on the mesh size.

When plotting the calculated values for the surfaces (τ_a, p_{max}) of a specimen geometry, in a graph of τ_a versus p_{max}, the curves similar to Fig. 2 are obtained. For each geometry the experimental data adhere fairly well to a linear relationship. It would seem that the Dang Van criterion correctly accounts for the experimental data, but it cannot be considered as a general criterion, the relationship τ_a–p_{max} being geometry dependent.

If, in place of the calculated values of τ_a and p_{max} for the surface of the specimen, we plot the calculated values (τ_a^*, p_{max}^*) at some definite distance from the surface (depth) which depends upon the material, for instance, 50 μm for AFNOR 35CD4 steel with a tensile strength of 1000 MPa, the experimental data are regrouped and align themselves along a single straight line, whatever the specimen geometry. This line expresses the 'behaviour law' of the material

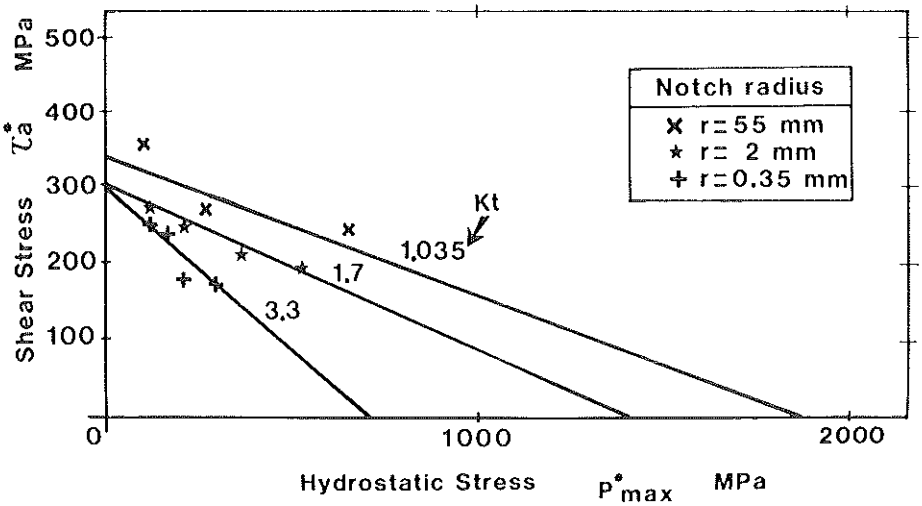

Fig 2 Calculated shear stress amplitude vs maximum hydrostatic stress for the surface at the fatigue limit of a 35CD4 steel

for unnotched specimens (Fig. 3). The off-line values are experimental results for cases where a macroscopic plastic strain occurred at the notch tip. Table 1 gives the depth of the critical layer CC, in μm, for various metals. These data were obtained using tension–compression fatigue test with a stress ratio $R = -1$ or $R = 0.1$ on notched specimens. The references of these tests are indicated in Table 1. Moreover, these data have been obtained from a small number of results and should be considered approximate, pending further work. Unfortu-

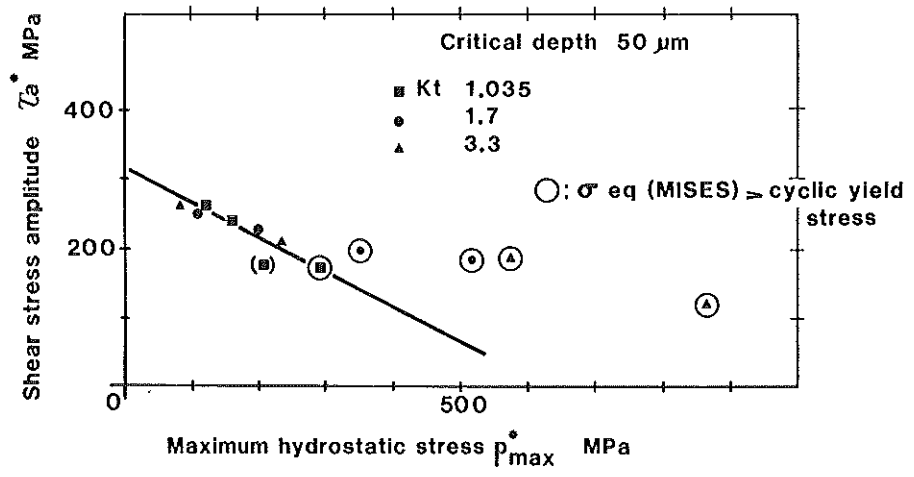

Fig 3 The shear stress amplitude vs maximum hydrostatic stress at a depth of 50 μm from the surface. Elastic analysis. AFNOR 35CD4 steel

Table 1 Reference data from which is calculated the critical layer (CC) depth

Metal (reference)	*Heat treatment*	*UTS (MPa)*	*CC (μm)*
XC38 (**15**)	Annealed	585	70
35CD4 (**14**)	Hard and tempered	915	50
		1000	50
		1500	40
35NCD16 (**17**)	Hard and tempered	1270	50
TA6V (**16**)	Ann. 730°C/2 h	1020	180
TA6VE2 (**16**)	Hard and tempered	1190	120
AU4G1 (**17**)	Hard and tempered	480	40
AZ5GU (**17**)	T7351	480	80
A7U4SG (**17**)	T651	480	80

nately these results cannot be compared with the grain size of the materials, because grain size is not indicated in the papers from which the results were obtained (**15**)–(**17**).

In order to take into account the physical mechanisms of crack initiation, particularly shearing of the crystallographic planes in a grain of metal, it would be advisable to consider mean values of the shear stress $\overline{\tau_a}$ and the hydrostatic stress $\overline{p_{max}}$. These mean values are averaged over the volume element from the surface to twice the critical depth; see Fig. 4.

When retracing the graph of $\overline{\tau_a}$ versus $\overline{p_{max}}$ for the depth giving the best alignment of the data, the values obtained for these depths are similar to the values in Table 1 within an approximation range of two (Fig. 5), due to the

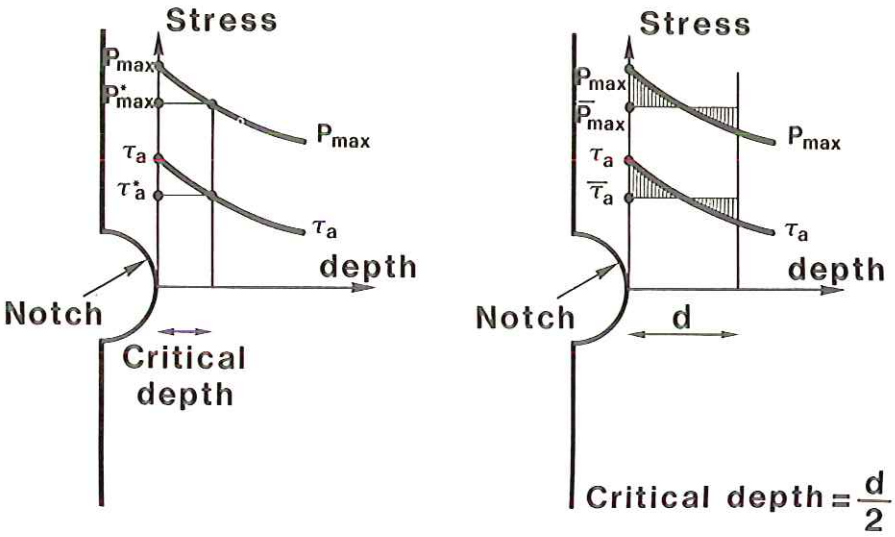

Fig 4 Procedure to determine mean values of shear stress amplitude $\overline{\tau_a}$ and maximum hydrostatic pressure, p_{max}

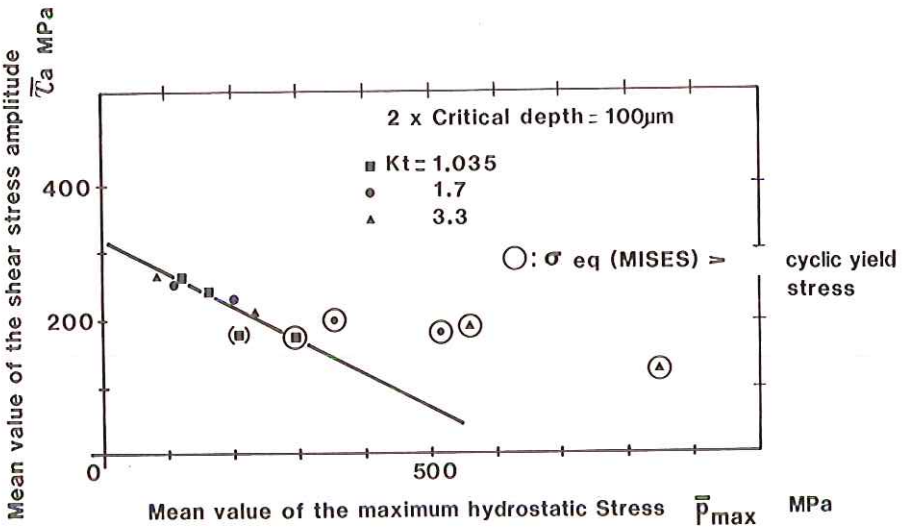

Fig 5 The shear stress amplitude vs hydrostatic stress using mean values averaged over the volume element from the surface to twice the critical depth. Elastic analysis. AFNOR 35CD4 steel

application of the mean values of $\overline{\tau_a}$ and $\overline{p_{max}}$. The critical depth may be more accurately determined by plotting the graph $\overline{\tau_a}$ versus $\overline{p_{max}}$ for various depths, and selecting the one which gives the best correlation coefficient, ϱ, and the least standard mean square deviation, σ^2, for the linear regression $\overline{\tau_a}$ versus $\overline{p_{max}}$ (Fig. 6).

When using the mean values $\overline{\tau_a}$ and $\overline{p_{max}}$, the critical depth will be defined as the half-thickness of the volume element giving the best fit of the experimental data with the fatigue data obtained on specimens without a stress concentration. If the Crossland criterion is used in place of the Dang Van criterion, plotting the representative points on a graph of $\overline{\tau_{oct,a}}$ versus $\overline{p_{max}}$ will give the best alignment of data for same values of the critical layer depth. The Dang Van criterion will, however, give a better correlation for the alignment of the experimental data.

The value of the critical depth will be different according to the material concerned. The calculated critical depth depends upon the microstructure. It is approximately 70 μm for an XC 38 steel in the annealed condition, larger than for hardened and tempered 35CD4 and 35NCD16 steels whose microstructures are finer.

It should be noted that, for a 35CD4 steel heat-treated to a tensile strength of 1500 MPa, the value of 40 μm for the calculated critical layer depth is less than for the same steel heat-treated to give a tensile strength of 1000 MPa, where it is 50 μm. It seems logical that the concept of a critical layer is related to microstructure. Stieler has already mentioned that the depth of that layer

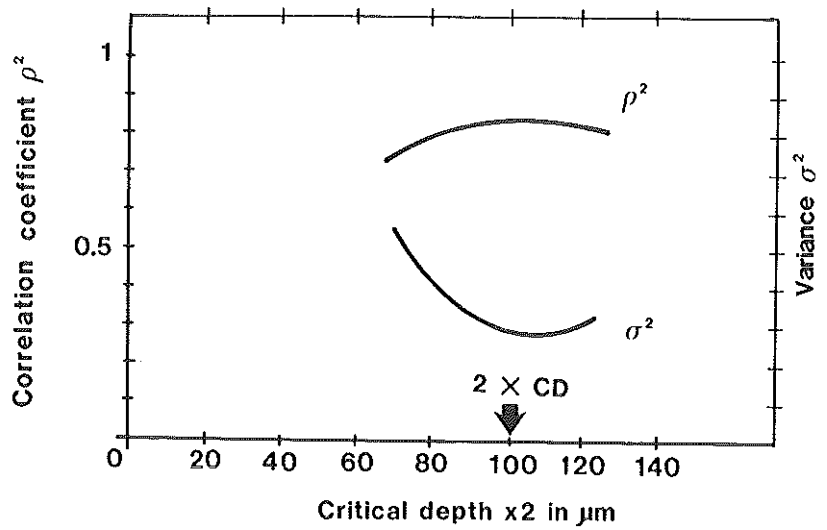

Fig 6 Determination of the critical layer depth for 35CD4 steel with the correlation coefficient and the standard mean square deviation

should be of the size of a grain, and this would be justified if we consider that slip must affect at least one grain in order to initiate damage.

Unfortunately, the microstructure of quenched and tempered steels is complex and various features can be defined for these steels, all of different sizes, e.g., laths, plates, packets, prior austenite grains, etc.

Plastic strain at the notch tip

In the foregoing analysis, we have neglected the experimental results that imply macroscopic plastic strain at the notch tip, which produce a Von Mises equivalent stress larger than the cyclic yield stress of the metal. The cyclic plastic strain alters the stress state in the critical zone. As a result the maximum hydrostatic stress is altered due to the plastic deformation, while the shear amplitude remains unchanged (**2**). Computation by the finite element method (CETIM software) for the elastoplastic conditions can provide the new stress distribution (Fig. 7). Introducing the data from a simple tensile test on steel we obtain a lower value with respect to the computation for the elastic state (Figs 7 and 8). This first computation is not suitable for taking into account the cyclic plastic strain at the tip of the notch.

An iterative computation including the strain-hardening law over a sufficient number of cycles must be made to obtain the stress state after elastic shakedown, but it is a long and costly procedure. Zarka and Casier (**18**) have suggested a simplified method using a linear kinematic hardening model, which gives, within a short time, an approximate value of the stresses under stabilized

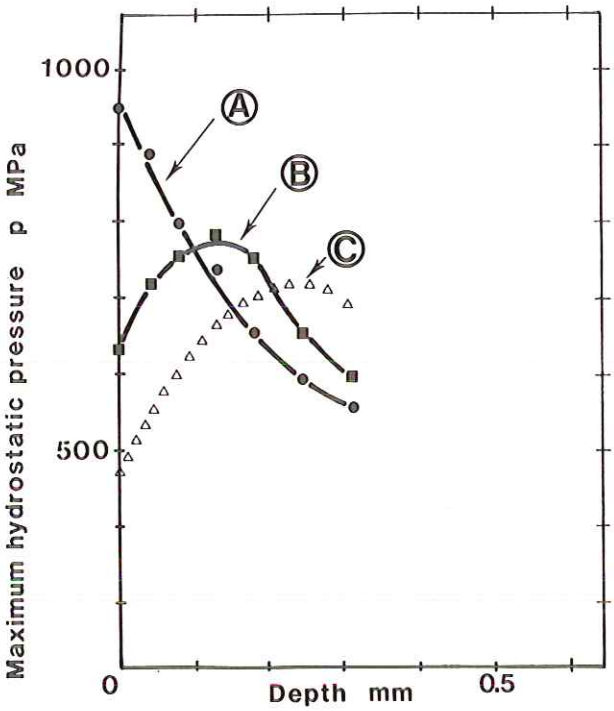

Fig 7 Variation of the maximum hydrostatic stress with depth. Mean stress = 500 MPa and K_t = 3.3 for 35CD4 steel. A = elastic; B = elasto-plastic (monotonic stress–strain curve); C = elasto-plastic (cyclic stress–strain curve)

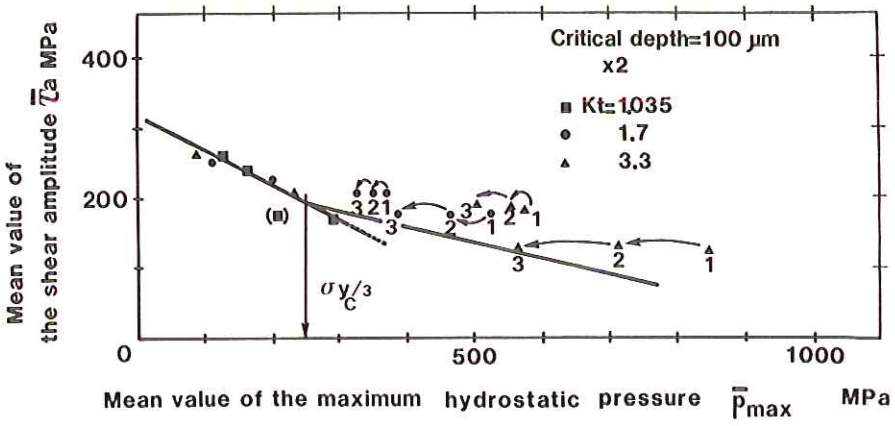

Fig 8 The shear stress amplitude vs maximum hydrostatic stress, taking into account the plastic strain at the notch tip. (Mean values integrated over the volume element to twice the initial depth.) 1 – elastic analysis, 2 – elasto-plastic analysis (monotonic stress–strain curve), 3 – elasto-plastic analysis (cyclic stress–strain curve)

cycling. Introducing the cyclic-hardening curve into the computation, the new procedure gives new values for $\overline{p_{max}}$ (Figs. 7 and 8). By taking into account cyclic strain-hardening, the previously outlying data comes closer to the intrinsic curve of the material. These data, however, still do not correspond to the intrinsic behaviour law of the material for the elastic field. It may be assumed that, in the case of confined plastic strain, the data points representing the material behaviour are obeying a specific law in the approximate stress range $p_{max} > \sigma_{y,c}/3$. Further work should define an equation for this condition using an equation for elastic behaviour of the form $\overline{\tau_a} + \overline{\alpha p_{max}} = \beta$ and a relationship for cyclic strain hardening.

Conclusion

An analysis of fatigue tests under tension–compression stressing on notched specimens has illustrated a critical depth that characterizes the microstructural state of various metals. Introducing this parameter into multiaxial criteria of fatigue, may explain fatigue behaviour for both complex stressing and stress gradients.

The concept of a 'critical depth' combined with a multiaxial fatigue criterion valid for non-proportional loading, such as the Dang Van or the Crossland modified criterion presented in reference (5), should result in a long-life fatigue criterion of general validity for any geometry and loading. Further work should be done to check the validity of such criteria for non-proportional loading, and to try to relate the concept of a critical depth with the microstructure of the metal and short crack initiation or a short crack arrest mechanism.

References

(1) GARUD, Y. S. (1981) Multiaxial fatigue: a survey of the state of the art, *J. Testing Evaluation*, **9**, 165–178.
(2) DANG, VAN, K. (1973) Fatigue strength of metals, *Sciences et techniques l'Armement*, **47**, 641–722.
(3) CROSSLAND, B. (1956) Effect of large hydrostatic pressure on the torsional fatigue strength of an alloy steel, *Proceedings of the International Conference on the Fatigue of Metals*, I. Mech. E., London, pp. 138–149.
(4) FUCHS, H. O. (1979) Fatigue research with discriminating specimens, *Fatigue Engng Mater. Structures*, **2**, 207–215.
(5) DANG VAN, K. and COLL, (1988) Criterion for high cycle fatigue crack initiation under multiaxial loading, *Proceedings of the Second International Conference on Multiaxial Fatigue*, Sheffield, December 1985.
(6) NEUBER, H. (1958) *Kerbspannungslehre*, Springer, Berlin, p. 158.
(7) HEYWOOD, R. B. (1962) *Designing against fatigue*, Chapman and Hall, London, p. 95.
(8) STIELER, M. (1954) *Untersuchungen über die Daverschwing festigkeit metallischer Bauteile bein Raumtemperatur*, Thèse de Dr Ingr., Technische Hochschule Stuttgart.
(9) DEVAUX, J. C., DESCATHA, Y., RABBE, P., and PELLISSIER-TANON, A. (1979) A criterion for analysing fatigue crack initiation in geometrical singularities, Fifth Conference SMIRT – Berlin, paper G8/1. 13–17/08/79.
(10) MATAKE, T. and IMAI, Y. (1980) Fatigue criterion for notched and unnotched specimens under combined stresses state, *ZAIRYO*, **29**, 993–997.
(11) MILLER, K. J. (1982) The short crack problem, *Fatigue Mater. Structures*, **5**, 223–232.

(12) MUTOH, Y. and RADHAKRISHNAN, V. M.-P. (1981) An analysis of grain size and yield stress effects on the fatigue limit and threshold stress intensity factor, *J. Engng Mater. Technol.*, **103**, 229–233.
(13) FLAVENOT, J. F. and SKALLI, N. (1983) Critical layer depth, a new approach for computing structures submitted to multiaxial stresses, *Mécanique Matériaux Electricité*, **397**, 15–25.
(14) POMEY, G. and RABBE, P. (1966) Etude de l'effet d'entaille sur le comportement à la fatigue d'un acier au Cr–Mo, *Revue de Métallurgie*, **63**, 579–996.
(15) BRAND, A. (1980) *Calcul des structures à la fatigue – Méthode du gradient*, CETIM, Senlis, France.
(16) AUVINET, J., LELEU, G., NOTTON, G., and MARQUIEZ, G. (1973) Caractéristiques mécaniques et de fatigue des alliages TA6V et TA6V6E2. *Mém. Scientifiques Revue Métallurgie*, **70**, 809–821.
(17) Essais de caractérisation de fatigue, *Procès-verbal CEAT* (Centre d'Etudes Aéronautiques de Toulouse) No. M67487, No. N3 557800, No. N2 478800.
(18) ZARKA, J. and CASIER, J. (1979) Elastic–plastic response of a structure to cyclic loading: practical rules, *Mechanics Today*, **6**, 93–198.